Interface Dissipative Mechanisms in an Elastomeric Matrix Reinforced with MWCNTs

Marco Aurilia,* Luigi Sorrentino, Salvatore Iannace

Dissipative mechanisms occurring at the interface between multiwall nanotubes (MWCNT) and an elastomeric matrix are investigated and quantitatively predicted through analytical equations derived from a micromechanical model. The effects of MWCNT aspect ratio on dissipative properties of the reinforced system are investigated at high strains (100–300%). Cyclic tensile tests illustrate that the fraction of dissipated strain energy increases with the amount of MWCNT and varies with their aspect ratio. Lower mean diameter MWCNT are able to dissipate a higher amount of strain energy. The model developed on the basis of the shear lag theory correctly predicts the dissipated strain energy at high strains, taking into account the different contributions to the mechanical behavior of nanotubes' different aspect ratios.

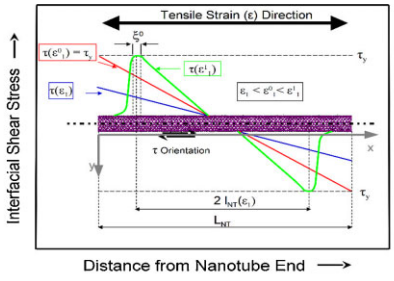

$$l_{NT} = \frac{2}{\beta}\tanh^{-1}\left(\frac{2\tau_y}{E_{NT}\varepsilon_1\beta R_{NT}}\right)$$

$$\beta = \sqrt{\frac{2G_m}{E_{NT}R_{NT}^2\ln\left(\frac{R}{R_{NT}}\right)}}$$

E_{NT} Nanotube Modulus
l_{NT} Length Nanotube
l_{NT} Length of Nanotube\Matrix Interface
R_{NT} Nanotube Radius
R Distance Between Nanotubes
ε_1 Composite Strain
τ_y Interfacial Shear Strength
ξ^0 Width of matrix surrounding the nanotube at which the shear stress is constantly equal to interfacial shear strength τ_y

1. Introduction

The exceptional properties of carbon nanotubes have boosted research activities in several application fields, ever more as their availability in different aspect ratios and surface functionalizations at reduced costs increases. Among all multiwall nanotubes (MWCNT) features, their very high mechanical properties have drawn the attention of researchers as reinforcement in polymeric materials. In fact, nanotubes have axial Young's modulus as high as 1 TPa, tensile strength ranging between 40 and 60 GPa, and strain at break of about 15%,[1] but their reinforcing efficiency crucially depends on both their dispersion and orientation in the host matrix.

In order to exploit such high mechanical contribution as polymer reinforcement, their geometry (in particular their aspect ratio) and interface properties must be properly designed to allow an effective reinforcement. For example, a polymeric matrix reinforced with aligned carbon nanotube 1 μm long and 10 nm in diameter, with an aspect ratio (L_{NT}/D_{NT}) equal to 100, should have an interfacial shear strength of ≈250 MPa in order to bring to failure nanotubes and deploy all their potential reinforcement, according to the Kelly-Tyson relation:[2,3]

$$\tau_i = \frac{\sigma_{NT} D_{NT}}{2L_{NT}} \quad (1)$$

where τ_i is the interfacial shear strength between nanotube and polymeric matrix, σ_{NT} is the tensile strength of the nanotube, D_{NT} and L_{NT} are nanotube's diameter and length, respectively. Such τ_i value (250 MPa) is considerably higher than polymer's tensile and shear strengths

M. Aurilia
IMAST – Technological District on Polymeric and Composite Materials Engineering and Structures, Piazza Bovio n. 22, Napoli 80133, Italy
E-mail: marco.aurilia@gmail.com
L. Sorrentino, S. Iannace
CNR-IMCB – National Research Council, Institute of Composite and Biomedical Materials, Piazzale Enrico Fermi, Località Granatello n. 1, Portici (Napoli) 80055, Italy

Macromol. Theory Simul. **2013**, *22*, 198–206

DOI: 10.1002/mats.201200070

(≈60–120 and ≈10–30 MPa, respectively[4]) and very difficult to be achieved at nanotube/polymer interface. A suitable strategy for effective reinforcement could be the dispersion of nanotubes with very high aspect ratio, e.g., 1 000, that could result in nanotube failure (not interface failure) with τ_i values not higher than 25 MPa, a definitively more suitable value for conventional polymeric systems. In this case the homogeneous dispersion of such high aspect ratio nanotubes is very challenging.[5,6]

Furthermore, proper tuning of interface properties is consequently fundamental in carbon nanotube-reinforced polymers to enhance the desired structural property, and by ranging the interfacial shear strength from very high to poor it is possible to influence the different aspects of the mechanical response of the composite structure. Many authors reported on polymeric systems reinforced with nanotubes which exhibited a poor adhesion with hosting matrix but presented both increased damping properties and enhanced elastic characteristics.[7–14] This increase in damping has been qualitatively attributed to the sliding interface between nanotubes and matrix, but it was investigated in small strain range (typically between 1 and 10%) because the reinforced matrices in most of these studied systems were rigid glassy or highly crosslinked polymers with low strain at break.[7–10,12,15]

Recent studies have shown that randomly oriented nanotubes are able to reinforce elastomeric matrices either in the elastic region (low strains) or at high strains (ultimate properties) and the improved reinforcing effect has been attributed to the increased orientation of nanotubes along the strain direction.[16]

In the current work, a thermoplastic elastomeric matrix filled with MWCNT have been produced and characterized. The influence of the nanotubes addition on stiffness, strength and on all dissipative phenomena of the elastomer have been investigated. Dissipative mechanism at interface nanotube/matrix have been evaluated in the tensile strain range 0–300% and interpreted with analytical equations derived from the shear lag theory,[3,17] which have shown that in a system reinforced by parallel discontinuous fibers the interface fiber/matrix, as strain increases, starts to fail at fibers ends, in turn contributing to dissipate part of the strain work. The derived equations allowed to relate the dissipative phenomena in the nanocomposites to both nanoparticles features (dimensions, volume fraction, and interfacial shear strength) and strain.

2. Experimental Section

A thermoplastic polyurethane – TPU (Desmopan DP 9370AU, shore hardness = 70 A, melt flow index = 35–55 cm^3/10 min), supplied by Bayer Gmbh (Leverkusen, Germany), has been used as elastomeric matrix. Two types of multiwalled carbon nanotubes have been dispersed in the polymeric matrix: NANOCYL™ NC3150 (average length <1.0 μm, average diameter = 9.5 nm) purchased by Nanocyl (Sambreville, Belgium) and Sigma–Aldrich 636509-2g (outer diameter 10–30 nm, inner diameter 5–10 nm, length 0.5–500 μm) purchased from Sigma–Aldrich (Spruce St. Louis, MO, USA). In the following nanotubes purchased by Nanocyl and Sigma–Aldrich will be referred to as NC-NT and SA-NT, respectively. MWCNT were ultrasonicated by a dipping tip sonicator (Misonix S3000, Farmingdale, NY, USA) for 60 min at room temperature in tetrahydrofuran – THF (0.1% volumetric solution of nanotube) with 18 W power. TPU pellets were then added to the ultrasonicated solution and mixed with a magnetic stirrer for 6 h. The solution was then poured in a Petri dish in order to allow THF evaporation at room temperature for 12 h and to obtain reinforced TPU films. Such films were further dried in a vacuum oven at 90 °C for 24 h. The dried films were cut and stacked to prepare 0.5 mm thick flat samples by hot pressing through a heated plates hydraulic press (model P 300P, Collin Gmbh, Ebersberg, Germany). TPU samples reinforced with 0.5, 5.0, and 20.0% by volume of SA-NT and with 0.1 and 5.0% by volume of NC-NT were prepared and stored for one month before testing.[16]

Scanning electron microscopy (SEM) analysis was performed with a Leica S440 (Leica Microsystems, Wetzlar, Germany) on the surface of TPU specimens in order to detect the orientation of MWCNT after tensile test. All sample surfaces were coated with gold layer before the observations to render conductive the specimen surface. Transmission electron microscopy (TEM) was carried out with a Philips EM 208 (Eindhoven, The Netherlands) at an acceleration voltage of 100 kV. The specimens for TEM analysis were prepared by microtoming 70-nm thick films from the TPU specimens with a LKB ultramicrotome. TEM images provided information about MWCNT dispersion in TPU matrix.

Specimens 50 mm long, 8 mm wide, and 0.5 mm thick were cut from films for the mechanical characterization. Tensile tests were performed by using an Instron 3310 universal testing machine (Norwood, MA, USA) with a cross-head speed of 50 mm · min^{-1} at room temperature. Load–unload cycles were carried out on TPU specimen at the same rate of tensile tests with progressively higher nominal strains (0.05, 0.1, 0.5, 1.0, 1.5, 2.0, 2.5, and 3.0) without dwell time when the straining changed direction. The specific work input (energy given to the system by stretching the nanocomposite) and the dissipated strain energy were obtained by integrating the load–unload stress–strain curves.[13,18] In particular, the integration of the curve in the load segment (line from point A to B of tensile test curve in Figure 1) returns the strain energy provided to the system as function of the strain and its value in correspondence of the maximum strain ε' before the unloading cycle has been taken as the specific work input at that strain. The specific work input to deform the material till the engineering tensile strain ε', W_{Tot}, has been determined according to the following equation:

$$W_{Tot}(\varepsilon') = \int_0^{\varepsilon'} \sigma d\varepsilon \quad (2)$$

where σ is the engineering tensile stress. The value of W_{Tot} in correspondence of the end point of unloading cycle ε_0 (point C' of the selected cycle in Figure 1 on W_{Tot} curve) has been taken as

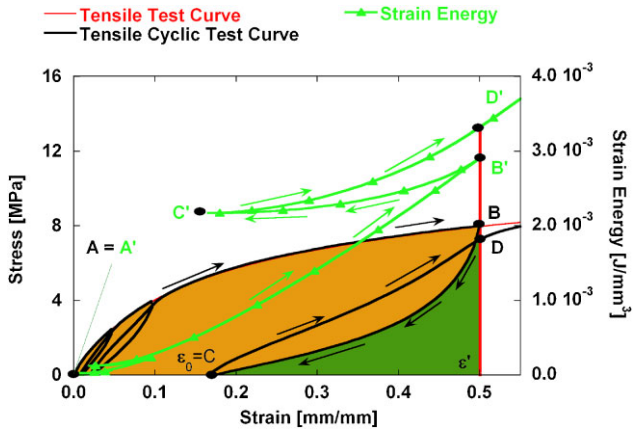

Figure 1. Cyclic stress–strain curve and its correlated strain energy.

dissipated strain energy at ε' strain, since it is the amount of the unrecovered strain energy upon unloading assuming that the contribution to dissipation in the stretch B–C is negligible.

3. Theoretical Model

An analytical model has been developed to calculate the slipping at nanotube/elastomer interface as function of strain starting from the shear lag theory for composites reinforced with aligned discontinuous fibers. In such a system, the applied tensile load is transferred to the reinforcement through the fiber/matrix interface by a shearing mechanism between fibers and matrix. The polymeric matrix has lower modulus and strength than the fibers, and, as a result, the longitudinal strain parallel to the fibers is higher in the matrix with respect to the adjacent fibers. The mismatch in longitudinal strains generates a shear stress distribution across the fiber/matrix interface, assuming a perfect bond between the two constituents. If the stress transfer at the fiber tips (end cross sections) and the interaction between the neighboring fibers are assumed negligible, the normal stress distribution in a discontinuous fiber by a force equilibrium analysis may be calculated.[3] When the matrix is in the elastic state and the fiber/matrix bond is still unbroken, the interfacial shear stress is not constant and varies along the fiber axis. Assuming that the matrix has the same strain as the composite it is possible to derive shear stress at the fiber/matrix interface along the length of a discontinuous fiber:[3,17]

$$\tau = \frac{1}{2} E_f \varepsilon_1 \beta R_f \frac{\sinh\beta\left(\frac{l_f}{2} - x\right)}{\cosh\beta\frac{l_f}{2}} \tag{3}$$

with

$$\beta = \sqrt{\frac{2G_m}{E_f R_f^2 \ln\left(\frac{R}{R_f}\right)}} \tag{4}$$

where E_f is the elastic modulus of fibers, ε_1 is the longitudinal engineering strain in the composite (defined as $\varepsilon_1 = (L - L_0)/L_0$, where L and L_0 the actual elongation and initial length of the composite, respectively), and G_m is the matrix shear modulus, x is the abscissa (coincident with nanotube axis with the origin in the left end), R_f the fiber radius and R is the center-to-center distance from a fiber to its nearest neighbor.

In elastomeric systems reinforced with MWCNT the huge difference between the elastic moduli of matrix and MWCNT results in a steep increase in the shear stress at TPU/MWCNT interface as the composite strain increases. In the case of the TPU, there are points along the nanotube axis where the shear stress start to exceed typical interfacial shear strength (ranging between 0.5 and 14.0 MPa[16]) already at 0.05 strain, as illustrated in Figure 2.

The graph in Figure 2 allows to define the distance from the nanotube end at which the shear stress equals the interface strength. This point is the intersection between the horizontal line, representing the TPU interface strength (two very different interfacial shear strength values were used as references), and the curve derived from Equation (2), which calculates the theoretical shear stress at the nanotube/TPU interface as function of the distance from the nanotube end. Slipping can occur along the stretches from the nanotube end to the intersection point, if present. Curves in Figure 2 were calculated for two MWCNT contents (0.1 and 5.0 vol.-%), at two strains (0.05% and 1.0%) by setting the nanotubes length to 1 000 nm and their radius equal to 4.75 nm, the modulus of the matrix E_m equal to 6.57 MPa (evaluated from the stress–strain curve of the

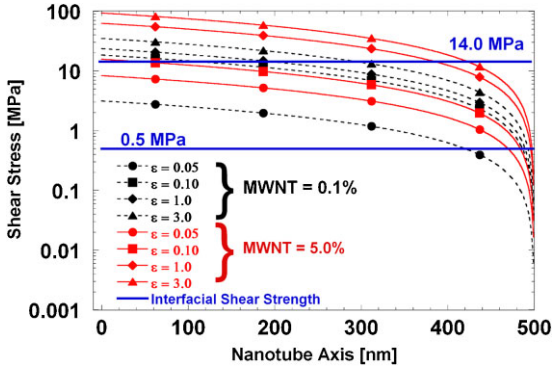

Figure 2. Shear stress at nanotube/matrix interface along nanotube axis in reinforced systems with different nanotube content at several strains.

investigated TPU), $G_m = E_m/2(1+\nu)$ with the Poisson's ratio ν equal to 0.4 (due to the low strains considered).

In Equation (2) the fiber/matrix bond is supposed to be perfect, but it drastically reduces or fails when the interfacial shear stress exceeds, with the increasing of the strain, either shear yield stress of the matrix or bonding strength of the fiber/matrix interface.[19] By inverting Equation (2), it is possible to derive the nanotube/matrix interface length l_{NT} as function of ε_1 (as the distance from the nanotube center) along which the stress does not exceed the interfacial shear strength (see Figure 3), taking into account that the shear stress is highest at nanotube ends ($x = 0$)[3]:

$$l_{NT} = \frac{2}{\beta}\tanh^{-1}\left(\frac{2\tau_y}{E_{NT}\varepsilon_1\beta R_{NT}}\right) \quad \text{for } 0 < \frac{2\tau_y}{E_{NT}\beta R_{NT}} < \varepsilon_1 \tag{5}$$

where E_{NT} and R_{NT} are the elastic modulus and radius of MWCNT, respectively.

The difference between L_{NT} and l_{NT} (ε_1) is the stretch of nanotube along which the shear stress at the interface exceeds interfacial shear strength τ_y, as shown in Figure 3. Assuming that this interface portion is not able to transfer the stress from the matrix to the nanotube it is possible to determine the elementary work performed to create this "loose" interface as:

$$dL_y = 2\pi R_{NT}\tau_y\xi^0 dx \tag{6}$$

where ξ^0 is the width of matrix surrounding the nanotube (Figure 3) at which the shear stress is constantly equal to interfacial shear strength τ_y and dx is the infinitesimal increment of "loose" interface along nanotube axis due to infinitesimal increment of the strain $d\varepsilon_1$. The latter can be determined by differentiation of the difference between the half of nanotube length $L_{NT}/2$ and the distance $l_{NT}/2$:

$$\begin{aligned} dx &= d\left(\frac{L_{NT}}{2} - \frac{l_{NT}}{2}\right) = d\left(\frac{L_{NT}}{2} - \frac{1}{\beta}\tanh^{-1}\left(\frac{2\tau_y}{E_{NT}\varepsilon_1\beta R_{NT}}\right)\right) \\ &= -\frac{1}{\beta}d\left(\tanh^{-1}\left(\frac{2\tau_y}{E_{NT}\varepsilon_1\beta R_{NT}}\right)\right) \\ &= -\frac{1}{\beta}\frac{1}{1-\left(\frac{2\tau_y}{E_{NT}\varepsilon_1\beta R_{NT}}\right)^2}\frac{2\tau_y}{E_{NT}\beta R_{NT}}\frac{-1}{\varepsilon_1^2}d\varepsilon_1 \end{aligned} \tag{7a}$$

$$dx = \frac{2\tau_y}{E_{NT}\beta^2 R_{NT}}\frac{1}{\varepsilon_1^2 - \left(\frac{2\tau_y}{E_{NT}\beta R_{NT}}\right)^2}d\varepsilon_1 \tag{7b}$$

The work L_y performed at nanotube interface to yield the whole "loose" interface can be evaluated as integral of the combined Equation (6) and (7b), as function of the composite's strain ε_1, from the strain value ε_1^0, at which l_{NT} is equal to L_{NT}, to the final strain value ε_1^f:

$$\begin{aligned} L_y(\varepsilon_1) &= \int_{\varepsilon_1^0}^{\varepsilon_1^f} 2dL = \int_{\varepsilon_1^0}^{\varepsilon_1^f} 4\pi R_{NT}\tau_y\xi^0\frac{2\tau_y}{E_{NT}\beta^2 R_{NT}}\frac{1}{\varepsilon_1^2 - \left(\frac{2\tau_y}{E_{NT}\beta R_{NT}}\right)^2}d\varepsilon_1 \\ &= \int_{\varepsilon_1^0}^{\varepsilon_1^f}\frac{8\pi\tau_y^2\xi^0}{E_{NT}\beta^2}\frac{1}{\varepsilon_1^2 - \left(\frac{2\tau_y}{E_{NT}\beta R_{NT}}\right)^2}d\varepsilon_1 \\ &= \left[\frac{8\pi\tau_y^2\xi^0}{E_{NT}\beta^2}\left(-\frac{E_{NT}\beta R_{NT}}{2\tau_y}\right)\tanh^{-1}\left(\frac{\varepsilon_1 E_{NT}\beta R_{NT}}{2\tau_y}\right)\right]_{\varepsilon_1^0}^{\varepsilon_1^f} \\ &= \left[-\frac{4\pi\tau_y\xi^0 R_{NT}}{\beta}\tanh^{-1}\left(\frac{\varepsilon_1 E_{NT}\beta R_{NT}}{2\tau_y}\right)\right]_{\varepsilon_1^0}^{\varepsilon_1^f} \quad \text{when } \varepsilon_1 < \frac{2\tau_y}{E_{NT}\beta R_{NT}} \end{aligned} \tag{8a}$$

or

$$= \left[-\frac{4\pi\tau_y\xi^0 R_{NT}}{\beta}\coth^{-1}\left(\frac{\varepsilon_1 E_{NT}\beta R_{NT}}{2\tau_y}\right)\right]_{\varepsilon_1^0}^{\varepsilon_1^f} \quad \text{when} \quad \varepsilon_1 > \frac{2\tau_y}{E_{NT}\beta R_{NT}} \tag{8b}$$

$$\varepsilon_1^0 = \frac{2\tau_y}{E_{NT}\beta R_f}\coth\left(\beta\frac{L_{NT}}{2}\right) \tag{8c}$$

$$= 2\pi\tau_y\xi^0 R_{NT}L_{NT} - \frac{4\pi\tau_y\xi^0 R_{NT}}{\beta}\coth^{-1}\left(\frac{\varepsilon_1^f E_{NT}\beta R_{NT}}{2\tau_y}\right) \tag{8d}$$

Equation (8a–8d) allow to calculate the work performed to create a loose interface between matrix and nanotube as the axial strain in aligned nanotube direction increases. It is worth to point out that the first term of Equation (8d) is the work for the complete slipping of a single MWCNT from the surrounding matrix; the total work is calculated starting from the strain value (ε_1^0) at which shear stress at nanotube endings is equal to interfacial shear strength.

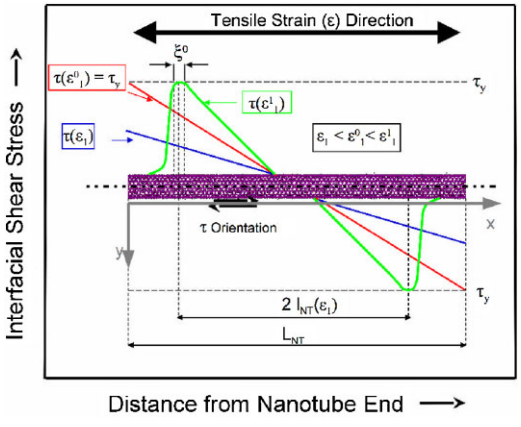

Figure 3. Interfacial shear stress at nanotube/matrix interface as composite strain increases.

4. Results and Discussion

In this section experimental evidences of the capability to dissipate mechanical energy at large strains through the nanotubes addition into TPU will be presented and the theoretical model derived in the previous section will be adapted to estimate the increment of dissipative phenomena at high strains when two types of nanotubes, differing for their aspect ratio distribution, are used as reinforcing phase. TEM images of TPU reinforced with both SA-NT and NC-NT show that MWCNT are singularly dispersed into the matrix (Figure 4).

The dispersion of MWCNT into the elastomeric matrix led to an increase of both modulus and strength with a negligible reduction in the ductility at low nanotubes content,[16,20,21] as confirmed by tensile test curves of prepared samples (Figure 5A and 5B). The sample reinforced with 5.0% NC-NT presented the highest increase in mechanical properties with respect to the neat TPU. The elastic modulus of the sample reinforced with 20% of SA-NT is comparable to that of 5.0% NC-NT sample, but its strain to failure was definitively reduced.

The fraction of strain energy dissipated has been measured through tensile cyclic tests. The comparison of cyclic load/unload tests with standard tensile tests has shown that the envelope of the loading portion of cyclic tests quite overlap with the non-cyclic one, indicating that in the investigated strain range either neat TPU or reinforced TPU samples are not affected by load/unload cycles at higher progressive strains (Figure 5C). This behavior permits to assume that dissipated strain energy calculated as the un-recovered energy in the load/unload cycle is a fraction of the specific work input measured in plain (non-cyclic) tensile test.[13,19] The fraction of dissipated strain energy in neat TPU and TPU + 0.1% NC-NT samples is almost similar and a slight increase in the reinforced sample is detected at high specific work input values (Figure 6). The sample reinforced with 5.0% of NC-NT presents a substantial increase of dissipated strain energy with respect to that of neat sample (ranging from 18 to 44%). Plain and cyclic tensile tests of elastomeric samples reinforced with SA-NT presented a trend analogous to that exhibited by NC-NT nanocomposites but with lower increments with respect to the neat polymer.

In order to estimate the contribution to strain energy of each component it is convenient to express the specific work input done to deform the TPU reinforced with MWCNT in the tensile test as sum of the strain energy contribution of each component, namely matrix, MWCNT and their interface:

$$W_{\mathrm{Tot}}(\varepsilon_1) = W_{\mathrm{m}}(\varepsilon_1) + W_{\mathrm{MWCNT}}(\varepsilon_1) + W_{\mathrm{I}}(\varepsilon_1) \tag{9}$$

where W_{m}, W_{MWCNT}, and W_{I} are strain energies stored and/or dissipated in the matrix, nanotubes, and the work performed at interface, respectively. To further elaborate Equation (9) and estimated its dissipative components, some assumptions have been done:

(1) The strain energy stored by nanotubes is prevalently due to elastic strain and its dissipative component may be neglected at high strain. In fact, the stress transfer from the matrix to the nanotubes is limited by the high mismatch between matrix and nanotube moduli as well as by the interfacial shear strength value.
(2) The dissipative strain energy component of the matrix is not affected by the nanotubes. This assumption may lead to a very small accuracy in the evaluation of dissipated strain energy within elastic region (lower than 100%). Nevertheless recent studies have shown that the addition of rigid rods such as nanotubes in an incompressible matrix (Poisson's ratio = 0.5) does not result in a Poisson's ratio variation, hence upon yielding of neat and reinforced TPUs (100% strain and Poisson's ratio approached the 0.5 value) the tensional states in the matrices of both reinforced and unreinforced systems should be comparable.[22] The implications of such assumptions will be further verified on the base of model fitting results.

Taking into account the assumptions (1) and (2), the dissipative strain energy components of Equation (9) may be written as:

$$W^{D}_{\mathrm{Tot}}(\varepsilon_1) = (1-\phi_{\mathrm{MWCN}})W^{D-\mathrm{neat\,TPU}}_{\mathrm{m}}(\varepsilon_1) + W^{D}_{\mathrm{I}}(\varepsilon_1) \tag{10}$$

As stated by other authors,[16,20] and illustrated by SEM image of TPU 5% SA-NT surface after tensile test (Figure 7), in elastomeric systems reinforced with MWNCT, nanotubes result to be significantly aligned in the strain direction as strain exceed 100% value (a sketch of the alignment mechanism is reported in

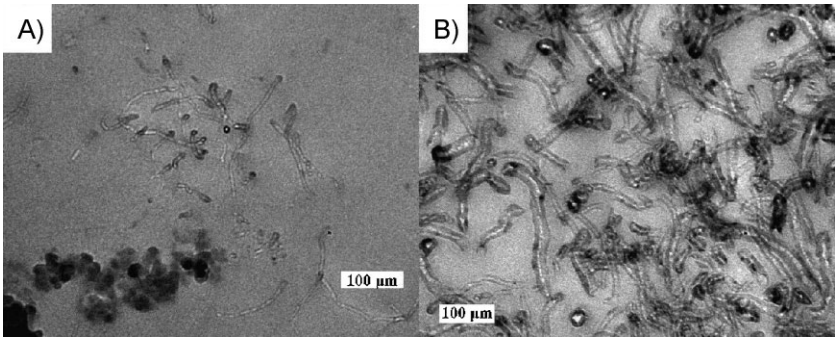

Figure 4. TEM images of TPU 5%NC-NT (A) and of TPU 5%SA-NT (B).

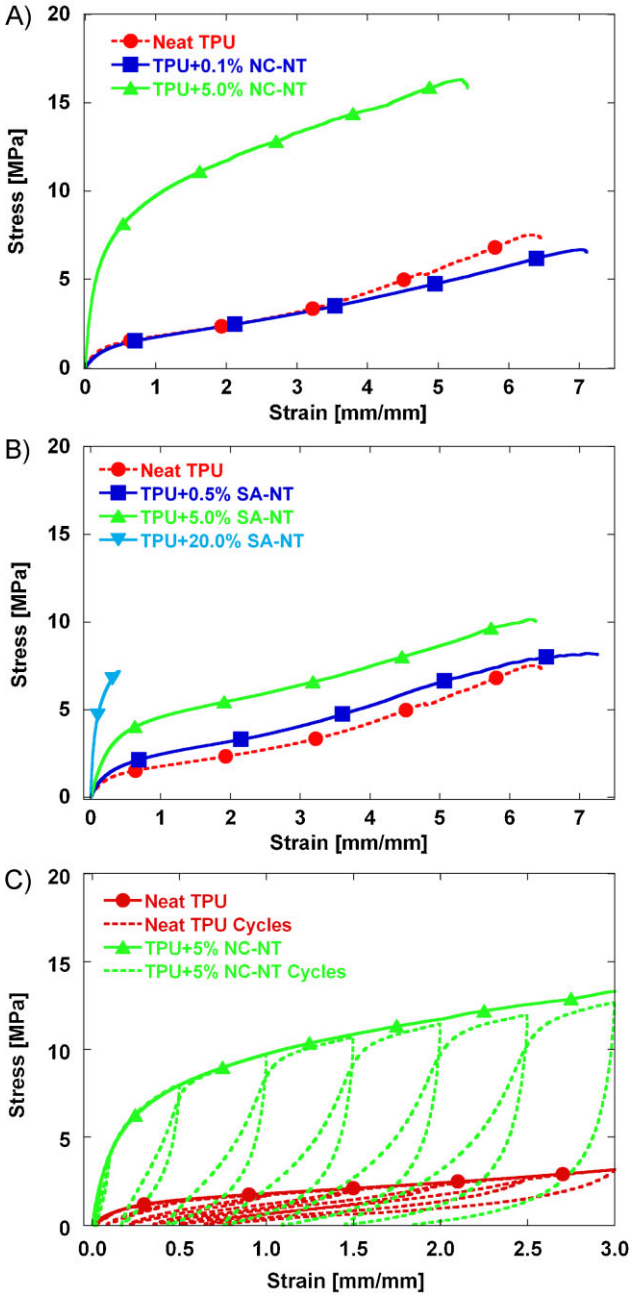

Figure 5. (A) Tensile test curves of neat TPU, TPU + 0.1% NC-NT, and TPU + 5.0% NC-NT; (B) tensile test curves of neat TPU, TPU + 0.5% SA-NT, TPU + 5.0% SA-NT, and TPU + 20.0% SA-NT; (C) load–unload test curves of neat TPU and TPU + 5.0% NC-NT.

Figure 8); this implies that Equation (8) can be used to determine the strain energy dissipated at the TPU/MWCNT interface starting from 100% strain.

For large strains, the mean distance between nanotubes and the matrix modulus vary, consequently the term β of Equation (3) is not constant during deformation, but it can be intended as an averaged value in the strain range and selected as a fitting parameter. Combining Equation (8)

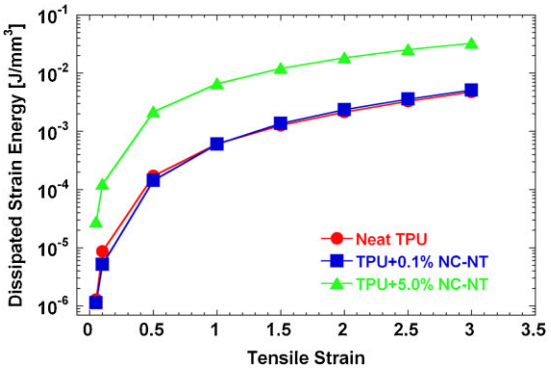

Figure 6. Dissipated strain energy as function of tensile strain of samples TPU, TPU + 0.1% NC-NT, and TPU + 5.0% NC-NT.

and 10, the dissipative fraction of the specific total work follows as (for the sake of simplicity Equation (8d) was utilized to develop the expression):

$$W^{D}_{\mathrm{Tot}}(\varepsilon_1) = (1-\phi_{\mathrm{MWCN}})W^{D-\mathrm{neat\,TPU}}_{\mathrm{m}}(\varepsilon_1) + \frac{\phi_{\mathrm{MWCNT}}}{V_{\mathrm{MWCNT}}} \times \left[2\pi\tau_{\mathrm{y}}\xi^{0}R_{\mathrm{NT}}L_{\mathrm{NT}} - \frac{4\pi\tau_{\mathrm{y}}\xi^{0}R_{\mathrm{NT}}}{\beta}\coth^{-1}\left(\frac{\varepsilon^{\mathrm{f}}_{1}E_{\mathrm{NT}}\beta R_{\mathrm{NT}}}{2\tau_{\mathrm{y}}}\right)\right] \tag{11}$$

This modified equation has been used to fit the model with experimental data according to the following equivalences:

$$W^{D}_{\mathrm{I}}(\varepsilon_1) = \frac{\phi_{\mathrm{MWCNT}}}{V_{\mathrm{MWCNT}}}\left[2\pi\tau_{\mathrm{y}}\xi^{0}R_{\mathrm{NT}}L_{\mathrm{NT}} - \frac{4\pi\tau_{\mathrm{y}}\xi^{0}R_{\mathrm{NT}}}{\beta}\coth^{-1}\left(\frac{\varepsilon^{\mathrm{f}}_{1}E_{\mathrm{NT}}\beta R_{\mathrm{NT}}}{2\tau_{\mathrm{y}}}\right)\right] = W^{D}_{\mathrm{Tot}}(\varepsilon_1) - (1-\phi_{\mathrm{MWCN}})W^{D-\mathrm{neat\,TPU}}_{\mathrm{m}}(\varepsilon_1) \tag{12}$$

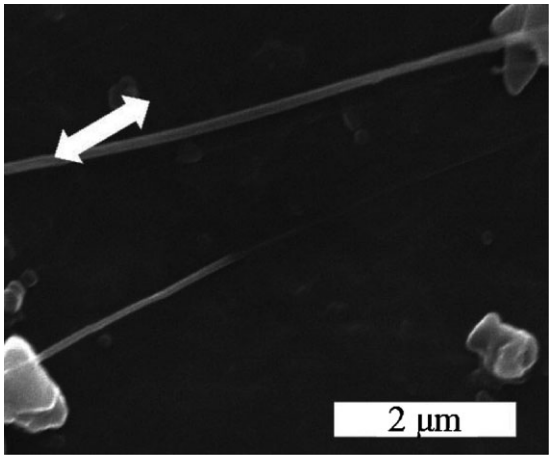

Figure 7. SEM image of TPU 5% SA-NT surface after tensile test (the arrow indicates the strain direction). It is evident the nanotube is straight and has slipped within the matrix creating a track.

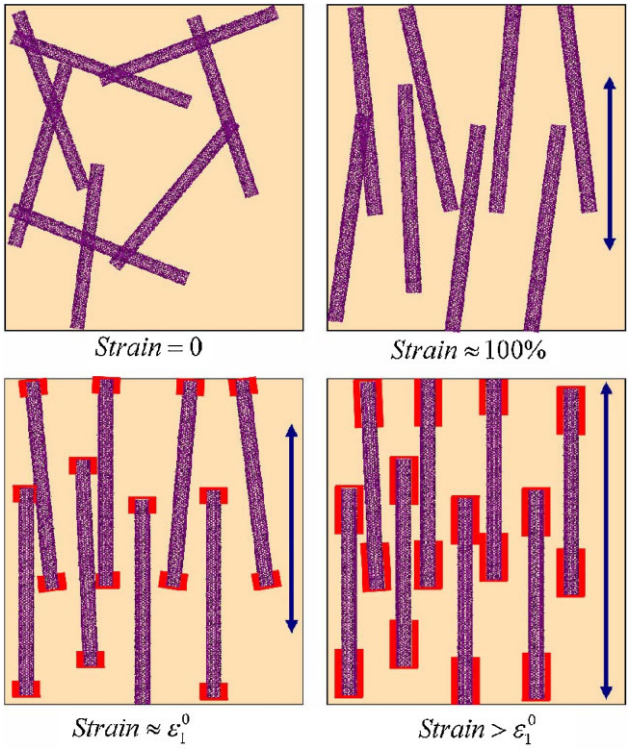

Figure 8. Alignment of nanotubes and loose interface formation and increase at different strains; the blue shows the direction and the intensity of the strain.

The second term of Equation (12) has been fitted to the difference of dissipative component of specific total work of reinforced system and the dissipative component specific total work of neat TPU samples (third term of the equation) as shown in Figure 9. The analytical curves approach experimental values at strains higher than 150%. This behavior derives from the assumptions on which the model has been developed: (a) that the interface between nanotube and polymeric matrix starts to fail at ε_1^0 (as reported in Table 1) and (b) that the dissipative contribution of the matrix is not influenced by the presence of nanotubes in the matrix. The latter yields higher error at low strain in the evaluation of last term of Equation (12), leading to neglect the complex tensional state that may establish in the matrix' region surrounding nanotubes, which in turn also induces local three dimensional strains values and results in higher strain energy dissipation.[23,24] This relevant issue has been tackled by other authors.[25,26]

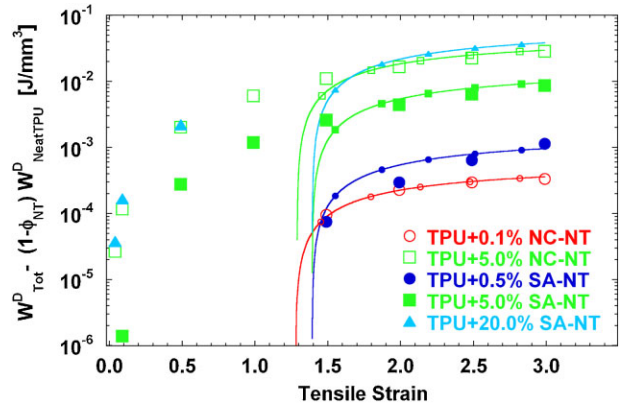

Figure 9. Experimental values of dissipated strain energy at interface nanotube/matrix (symbols) at different MWCNT contents as function of strain, and their fitting curves through Equation (11) (solid lines). The fitting parameters used in the model are reported in Table 1.

The parameters β, τ_y, ξ^0, and L_{NT}, selected as fitting variables, in addition to the values of the other model's parameters (taken from datasheets) are reported in Table 1. The values of β obtained by data fitting are higher in NC-NT samples, in agreement with their lower nanotube diameter with respect to SA-NT. The reduction of L_{NT} for NC-NT samples with the increase of their fraction is consistent with either experimental evidence that has shown the mean nanotubes length reduces as a consequence of processing,[27] or theoretical estimation of nanotube free length ($L_{NT}' \approx 2R_{NT}/\varphi_{NT}$) in a random 3D network of rigid rods.[28] The fitting value of the interfacial shear strength τ_y is considerably higher than either the values reported in literature (0.5–14.0 MPa[16]) or the shear yielding of TPU itself (0.33 MPa ≈ tensile yielding/$3^{0.5}$, from the Tresca criterion). This parameter must be considered as mean value over the investigated strain range and its value may increase over the yielding point (≈100% tensile strain) due to isostatic pressure around aligned nanotubes. Furthermore the assumptions that the dissipative component of the work performed to align nanotube in strain direction is negligible and that upon yielding the strain dissipated by the matrix is not affected by the nanotubes may lead to overestimate τ_y.

The developed system of equations accurately predicted the amount of the dissipated strain energy in the prepared nanocomposites at elevated deformations. It further highlighted that dissipated energy increases with nanotubes content and with the parameters τ_y (interfacial shear strength) and ξ^0 (stretch of the matrix/nanotube interface along which the shear stress is constantly equal to the interfacial shear strength), as well as with the decrease in nanotube diameter. Evidently, ξ^0 and τ_y are influenced by chemical and physical properties of both nanotube and hosting matrix. In addition, the fitting procedure has shown that the developed model is able to well fit experimental results and to predict the different effects that geometrical features of nanotubes, namely diameter and length, have on dissipated strain energy.

Table 1. Parameters and fitting parameters (fit. param.) used for fitting data with Equation (11).

MWCNT (vol.-%)	MWCNT type	E_{NT} (TPa)	R_{NT} (nm)	τ_y (MPa) fit. param.	ξ^0 (nm) fit. param.	L_{NT} (nm) fit. param.	β (nm^{-1}) fit. param.	ε_1^0
0.1	Nanocyl	0.6	4.75	50	50	750	2.1×10^{-4}	1.2921
5.0	Nanocyl	0.6	4.75	50	50	700	2.8×10^{-4}	1.3011
0.5	Sigma–Aldrich	0.6	16.75	60	50	3500	0.7×10^{-4}	1.4301
5.0	Sigma–Aldrich	0.6	16.75	60	50	3500	0.7×10^{-4}	1.4301
20.0	Sigma–Aldrich	0.6	16.75	60	50	3500	0.7×10^{-4}	1.4301

It is worth to highlight that the nanoube diameters (9.5 nm in MWCNT from Nanocyl, 10–30 nm for those from Sigma–Aldrich) is of the same order of magnitude of TPU hard domains average distance (10–15 nm)[29] as well as of the gyration radius of typical thermoplastic macromolecules. At such length scale it is questionable if consider the matter as continuous. However, since this aspect is very difficult to be estimated, the authors preferred to start with the hypothesis that continuum mechanics would be an acceptable assumption, relying the verification of this assumption on the parameter ξ^0 (the width of matrix surrounding the nanotube at which the shear stress may be considered constantly equal to the interfacial shear strength). The fitting procedure has provided a value for ξ^0 of 50 nm that is about two to five times grater than hard domains distance. This value is high enough to ensure that over such range the interaction matrix/nanotubes can be considered equal to a mean constant value, even if it could be locally variable within it. As a result, these considerations supported the choice to develop a system of equations based on the assumption that the interaction between TPU and MWCNT can be regarded within the framework of continuum mechanics.

In addition, the equations system can provide further insights into the toughening mechanism that nanotubes and/or graphene nanoplatelets induce in their nanocomposites, and can be used to quantify the different contributions to the dissipated energy in such systems. As an example, semicrystalline matrices have been reinforced with about 60% by volume of carbon nanotubes or graphene.[30–32] The measured toughness of those investigated systems (ranging from 570 to 970 $J \cdot g^{-1}$) was the sum of inelastic (dissipated) strain energy and elastic strain energy fraction released during materials failure. Equation (7) can account for the energy dissipated by the polymer/nanoparticle interface and by the matrix, estimating a value equal to 283.5 $J \cdot g^{-1}$ ($\tau_y = 30$ MPa, $\xi^0 = 30$ nm) at 300% strain, close to the strain to failure for those systems. The energy dissipated by nanotubes failure should also be considered since the higher matrix modulus (lower matrix/nanotubes modulus mismatch), and a rough estimation, from the equation $1/2 \cdot E_{NT}\varepsilon^2{}_{Rupture}\varphi_{NT}$ normalized by the nanotube density, leads to a value of 1764.70 $J \cdot g^{-1}$. This estimation is in excess and such value is based on the assumption that all available nanotubes in the matrix fail, but in real systems probably just a fraction of them reach the rupture but no quantification is available to be more precise. The three dissipative mechanisms (slip at interface matrix/filled, filler strain and rupture, matrix strain energy dissipation) can be estimated to predict the toughness enhancement of reinforced systems, and additionally they can be properly designed to create ad hoc high performance materials.

5. Conclusion

MWCNT dispersion in a polymeric matrix strongly increases the capability to dissipate mechanical energy at large strains through the nanotube/matrix interface slip due to the stiffness mismatch between the matrix itself and the reinforcement. Remarkably, an increase in the strain energy dissipation increase was measured in addition to typical mechanical properties improvements, namely Young's modulus and yield strength, they were obtained with a negligible decrease in strain to failure (except for very high nanotube content systems −20 vol.-%).

A theoretical model for the prediction of the energy dissipation at the MWCNT/TPU interface has been proposed. In particular, starting from assumptions made on dissipated strain energy in the matrix and on the alignment of nanotubes at high strains, a set of equations was derived. The analytical expressions successfully predicted the dissipated strain energy in nanocomposite systems as function of progressive strain in good agreement with experimental data. Furthermore, the model was also able to estimate the different contributions to the strain energy function of two types of MWCNT, differing for their geometry (length and diameter).

Acknowledgements: This study has been carried out with financial support from MIUR (Italy) within the FIRB project "MANTA," Prot. RBIP065YCL.

Received: October 1, 2012; Revised: November 27, 2012; Published online: February 18, 2013; DOI: 10.1002/mats.201200070

Keywords: elastomer; modeling; nanotubes; strain energy dissipation; thermoplastic polyurethane

[1] M. F. Yu, O. Lourie, M. J. Dyer, K. Moloni, T. F. Kelly, R. S. Ruoff, *Science* **2000**, *287*, 637.
[2] A. Kelly, W. R. Tyson, *J. Mech. Phys. Solids* **1965**, *195*, 329.
[3] P. K. Mallick, *Fiber Reinforced Composites*, 3rd edition, CRC Press, Taylor & Francis, Group, Boca Raton, Fl **2008**, p. 149.
[4] J. Brandrup, E. H. Immergut, E. A. Grulke, A. Abe, D. R. Bloch, *Polymer Handbook*, 4th edition, John Wiley and Sons, New York **1999**, p. V/17.
[5] M. R. Loos, K. Schulte, *Macromol. Theory Simul.* **2011**, *20*, 350.
[6] J. H. Du, J. Bai, H. M. Cheng, *eXPRESS Polym. Lett.* **2007**, *1*, 253.
[7] N. Koratkar, J. Suhr, A. Joshi, R. Kane, L. Schadler, P. Ajayan, S. Bartolucci, *Appl. Phys. Lett.* **2005**, *87*, 063102.
[8] J. Suhr, N. Koratkar, P. Keblinski, P. Ajayan, *Nat. Mater.* **2005**, *4*, 134.
[9] J. Suhr, N. Koratkar, *J. Nanosci. Nanotech.* **2006**, *2*, 483.
[10] J. Suhr, N. Koratkar, D.-X. Ye, T.-M. Lu, *Intell. Mater. Syst. Struct.* **2006**, *17*, 255.
[11] P. Ajayan, J. Suhr, N. Koratkar, *J. Mater. Sci.* **2006**, *41*, 7824.
[12] R. M. Lin, C. Lu, *Mech. Syst. Signal Proc.* **2010**, *24*, 2996.
[13] L. Ci, J. Suhr, V. Pushparaj, X. Zhang, P. M. Ajayan, *Nano Lett.* **2008**, *8*, 2762.
[14] P. M. Ajayan, J. M. Tour, *Nature* **2007**, *447*, 1066.
[15] J. Suhr, N. Koratkar, *J. Mater. Sci.* **2008**, *43*, 4370.
[16] B. Fernández-d'Arlas, U. Khan, L. Rueda, L. Martin, J. A. Ramos, J. N. Coleman, M. L. González, A. Valea, I. Mondragon, M. A. Corcuera, A. Eceiza, *Compos. Sci. Technol.* **2012**, *72*, 235.
[17] H. L. Cox, *Br. J. Appl. Phys.* **1952**, *3*, 72.
[18] C. P. Buckley, C. Prisacariu, C. Martin, *Polymer* **2010**, *51*, 3213.
[19] L. S. Schadler, C. Galiotis, *Inter. Mater. Rev.* **1995**, *40*, 3.
[20] F. Deng, M. Ito, T. Noguchi, L. Wang, H. Ueki, K. I. Niihara, Y. A. Kim, M. Endo, Q. S. Zheng, *ACS Nano* **2011**, *5*, 3858.
[21] B. Fernández-d'Arlas, U. Khan, L. Rueda, J. N. Coleman, I. Mondragon, M. A. Corcuera, A. Eceiza, *Compos. Sci. Technol.* **2011**, *71*, 1030.
[22] M. Das, F. C. MacKintosh, *Phys. Rev. E* **2011**, *84*, 061906.
[23] A. R. Payne, *J. Appl. Polym. Sci.* **1952**, *6*, 57.
[24] M. Aurilia, F. Piscitelli, L. Sorrentino, M. Lavorgna, S. Iannace, *Eur. Polym. J.* **2011**, *47*, 925.
[25] S. J. Hwang, R. F. Gibson, *Compos. Eng.* **1993**, *3*, 975.
[26] I. C. Finegan, R. F. Gibson, *Compos. Sci. Technol.* **2000**, *60*, 1077.
[27] E. T. Thostenson, T. W. Chou, *J. Phys. D: Appl. Phys.* **2003**, *36*, 573.
[28] R. C. Picu, *Soft Matter* **2011**, *7*, 6768.
[29] M. Aurilia, F. Piscitelli, L. Sorrentino, M. Lavorgna, S. Iannace, *Eur. Polym. J.* **2011**, *47*, 925.
[30] M. K. Shin, B. Lee, S. H. Kim, J. A. Lee, G. M. Spinks, S. Gambhir, G. G. Wallace, M. E. Kozlov, R. H. Baughman, S. J. Kim, *Nat. Commun.* **2012**, *3*, 1.
[31] A. B. Dalton, S. Collins, E. Muñoz, J. M. Razal, V. H. Ebron, J. P. Ferraris, J. N. Coleman, B. G. Kim, R. H. Baughman, *Nature* **2003**, *423*, 703.
[32] P. Miaudet, S. Badaire, M. Maugey, A. Derré, V. Pichot, P. Launois, P. Poulin, C. Zakriet, *Nano Lett.* **2005**, *5*, 2212.